Space-variant polarization manipulation for far-field polarimetry by use of subwavelength dielectric gratings

Yuri Gorodetski, Gabriel Biener, Avi Niv, Vladimir Kleiner, and Erez Hasman

Optical Engineering Laboratory, Faculty of Mechanical Engineering, Technion—Israel Institute of Technology, Haifa 32000, Israel

Received March 3, 2005; accepted April 15, 2005

A method for polarimetric measurement that uses a discrete space-variant subwavelength dielectric grating is presented. One retrieves the polarization state by measuring the far-field intensity of a beam emerging from the grating followed by a polarizer. The analysis for a partially polarized, quasi-monochromatic beam is performed by use of the beam coherence polarization matrix along with an extended van Cittert–Zernike theorem. We experimentally demonstrate polarization measurements of both fully and partially polarized light. © 2005 Optical Society of America

OCIS codes: 120.5410, 260.5430, 050.2770, 050.1960, 230.5440.

In recent years there has been considerable activity in applying optical polarimetry to a range of applications such as ellipsometry, bioimaging, and imaging polarimetry.[1] A commonly used method is to measure the time-dependent signal of a beam emerging from a rotating quarter-wave plate (QWP) followed by an analyzer and to then determine the polarization state by Fourier analysis. Increasing demands for faster and simpler methods has led to the development of the simultaneous four-channel polarimeter.[2] In this method the beam is split into four channels and each one is analyzed by use of different polarization optics. While this is being carried out, the real-time polarization state is calculated from the measured intensities. Unfortunately, implementations using this method are rather cumbersome, as they require multiple components.[3] Recently, Gori theoretically presented a new approach to polarimetry that makes use of a polarization grating composed of a space-variant polarizer.[4] The method was based on measuring the far-field intensity of the beam emerging from the grating. The analysis was performed using Jones calculus, which is suitable for fully polarized illumination.[5–7] Polarization gratings based on space-varying wave plates were also studied theoretically[5–7] and were experimentally demonstrated by use of subwavelength dielectric gratings.[5–7]

In this Letter we present, theoretically and experimentally, far-field polarimetry for fully and partially polarized light obtained by use of discrete space-variant subwavelength dielectric gratings (DSGs). To analyze partially polarized illumination we resort to the beam coherence polarization (BCP) matrix formalism on a helical basis, along with the extended van Cittert–Zernike theorem.[8] The proposed polarimeter is highly efficient as a result of using a DSG, which acts as a space-variant wave plate. Our polarimeter is a robust, passive, and compact system. The far-field polarimeter was fabricated by use of photolithographic techniques, thus making possible integration on a chip for biosensing applications.

The concept of our method is introduced in Fig. 1. A beam to be analyzed is incident upon the DSG, followed by a lens and a linear polarizer. The DSG splits the beam into three orders of different polarizations, which are focused by the lens into three separate spots. The polarization state of the incoming beam is determined by analyzing the three spots' intensities at two different orientation angles of the polarizer.

The analysis of our polarimetric approach for partially polarized quasi-monochromatic beams is conveniently performed by use of the BCP matrix analysis.[8] This formalism is derived from a more general case, the unified theory of coherence and polarization, which was investigated by Mandel and Wolf.[9] Assuming a beam propagating along the $\hat{z}$ axis, the BCP matrix for a plane at z = constant is defined as

$$\mathbf{J}(\boldsymbol{\rho}_1,\boldsymbol{\rho}_2,z)=\begin{bmatrix} j^{RR}(\boldsymbol{\rho}_1,\boldsymbol{\rho}_2,z) & j^{RL}(\boldsymbol{\rho}_1,\boldsymbol{\rho}_2,z) \\ j^{LR}(\boldsymbol{\rho}_1,\boldsymbol{\rho}_2,z) & j^{LL}(\boldsymbol{\rho}_1,\boldsymbol{\rho}_2,z) \end{bmatrix}, \quad (1)$$

where $j^{\alpha\beta}(\boldsymbol{\rho}_1,\boldsymbol{\rho}_2,z)=\langle E^{*}_{\alpha}(\boldsymbol{\rho}_1,z)E_{\beta}(\boldsymbol{\rho}_2,z)\rangle$, $\alpha,\beta=R,L$, and $\boldsymbol{\rho}_1$, $\boldsymbol{\rho}_2$ are the transverse position vectors of two arbitrary points in the plane. The angle brackets denote a time average, $E_{\alpha}(\boldsymbol{\rho},z)$ is the helical base component of the electric field, and R and L denote the

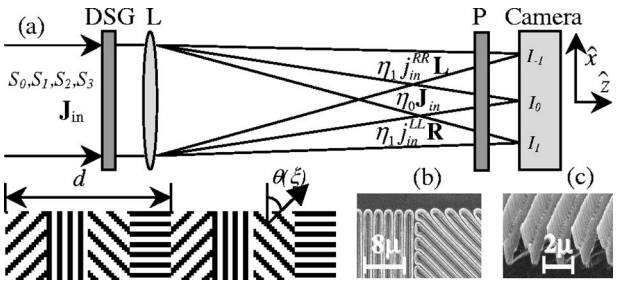

Fig. 1. (a) Schematic presentation of a far-field polarimetry based on a DSG followed by a Fourier lens (L) and a polarizer (P). Inset, magnified geometry of a DSG with a number of discrete levels N = 4. (b), (c) SEM images of the DSG, made on a GaAs wafer.

0146-9592/05/172245-3/$15.00

right- and left-handed circularly polarized (RCP and LCP, respectively) states.[8] In this Letter we analyze incident plane waves with uniform partially polarized distributions. In this case the incident beam's BCP matrix, $\mathbf{J}_{\text{in}}(\boldsymbol{\rho}_1,\boldsymbol{\rho}_2,z=0)$, has degenerated to a matrix of constant values. The BCP matrix just beyond the DSG was calculated as $\mathbf{J}_{\text{out}}(\boldsymbol{\rho}_1,\boldsymbol{\rho}_2,z=0)=\mathbf{T}^{\dagger}(\boldsymbol{\rho}_1)\mathbf{J}_{\text{in}}\mathbf{T}(\boldsymbol{\rho}_2)$, where $\mathbf{T}$ is the Jones matrix of the element[7] and the dagger denotes the Hermitian conjugate. The DSG behaves as a space-variant wave plate element with constant retardation and a space-varying fast axis, $\theta(\xi)$, along the ξ coordinate. The Jones matrix of such an element is given in the helical basis by[7]

$$\mathbf{T}=a\begin{bmatrix}1 & 0\\ 0 & 1\end{bmatrix}+b\begin{bmatrix}0 & \exp[i2\theta(\xi)]\\ \exp[-i2\theta(\xi)] & 0\end{bmatrix}, \quad (2)$$

where $a=[t_x+t_y\exp(i\phi)]/2$, and $b=[t_x-t_y\times\exp(i\phi)]/2$, t_x and t_y are the transmission coefficients for light polarized parallel and perpendicular to the subwavelength grooves, respectively, and ϕ is the retardation of the subwavelength grating. We assume the space-variant continuous groove orientation function to be $\theta(\xi)=(\pi\xi/d)|_{\text{mod }\pi}$, with period d along the ξ axis [Fig 1(a), inset]. The far-field BCP matrix of the beam emerging from the DSG, $\mathbf{J}_{ff}$, is calculated by use of the extended van Cittert–Zernike theorem for partially polarized beams.[8] Thus $j_{ff}^{\alpha\beta}(\mathbf{r}_1,\mathbf{r}_2,f)=A/\lambda^2f^2\iint j_{\text{out}}^{\alpha\beta}(\boldsymbol{\rho}_1,\boldsymbol{\rho}_2)K^*(\mathbf{r}_1,\boldsymbol{\rho}_1)K(\mathbf{r}_2,\boldsymbol{\rho}_2)\mathrm{d}^2\rho_1\times\mathrm{d}^2\rho_2$, with kernel $K=\exp[(-i2\pi/\lambda f)\mathbf{r}\boldsymbol{\rho}]$, where $A=\exp[i\pi(\mathbf{r}_2{}^2-\mathbf{r}_1{}^2)/\lambda f]$, $\mathbf{r}$ is the transverse position vector in the far-field plane, f is the focal length of the Fourier lens [Fig. 1(a)], and λ is the wavelength. As a result of the one-dimensional dependency of the DSG in the $\hat{x}$ direction, $\mathbf{r}_1$ and $\mathbf{r}_2$ reduce to x_1 and x_2, respectively. The calculation for the far-field BCP matrix yields $\mathbf{J}_{ff}(x_1,x_2,f)=A\big[\eta_0\delta(x_1)\delta(x_2)\mathbf{J}_{\text{in}}+\eta_1 j_{\text{in}}^{LL}\delta(x_1-\lambda f/d)\delta(x_2-\lambda f/d)\mathbf{R}+\eta_1 j_{\text{in}}^{RR}\delta(x_1+\lambda f/d)\delta(x_2+\lambda f/d)\mathbf{L}\big]$, where $\eta_0=|a|^2$ and $\eta_1=|b|^2$. $\mathbf{R}$ and $\mathbf{L}$ are the BCP matrix representation for the RCP and LCP states, respectively, where the matrix members are $R_{11}=1$, $R_{12}=R_{21}=R_{22}=0$ and, $L_{11}=L_{12}=L_{21}=0$, $L_{22}=1$ and δ is the Dirac delta function. From the calculated $\mathbf{J}_{ff}$ it is evident that the far-field BCP matrix comprises three polarization orders. The first converges to the point $x_1=x_2=0$ and maintains the incident BCP matrix. The second order is the RCP converging beam, with a spatial shift of $\lambda f/d$ in the x axis. The third order has a polarization direction and a spatial shift opposite those of the previous order. The shifts of the last two polarization orders result from a phase modification induced by the DSG. As this phase is created by a polarization manipulation by the DSG, it is geometric in nature.[5,6] Consider a RCP beam, $\mathbf{J}_{\text{in}}=\mathbf{R}$, incident upon a DSG with π retardation and transmission coefficients $t_x=t_y=1$. In such a case, $\eta_0=0$ and $\mathbf{J}_{ff}$ reduce to the LCP order alone, with a corresponding shift in the far field. LCP illumination also results in a single polarization order with opposite polarization and opposite shift in the far field. Identical results for the RCP and the LCP illumination were previously achieved using Jones calculus.[6,7] In a general case of a fully polarized incident beam, which is the coherent sum of the RCP and the LCP states, the BCP and Jones formalisms are in agreement. When the DSG is illuminated with unpolarized light, $\mathbf{J}_{\text{in}}$ becomes a unit matrix and the two shifted polarization orders, $\mathbf{R}$ and $\mathbf{L}$, calculated from $\mathbf{J}_{ff}$ result in equal efficiencies. This outcome indicates that the DSG acts on an unpolarized incident paraxial beam as if it were an incoherent superposition of RCP and LCP beams.

The far-field BCP after a polarizer is $\mathbf{J}_p=\mathbf{T}_p^{\dagger}(\gamma)\mathbf{J}_{ff}\mathbf{T}_p(\gamma)$, where $\mathbf{T}_p(\gamma)$ is the Jones matrix of a polarizer oriented at angle γ. The intensity of the beam emerging from the polarizer is calculated as the trace of $\mathbf{J}_p$ with $x_1=x_2$. The measured intensity is separated into three spots, which are located at $x=\lambda f/d$, $x=0$, and $x=-\lambda f/d$ with magnitudes of $I_{-1}=\eta_1(S_0-S_3)/4$, $I_0(\gamma)=\eta_0(S_0+S_1\cos 2\gamma+S_2\sin 2\gamma)/2$, and $I_1=\eta_1(S_0+S_3)/4$, respectively. S_0, S_1, S_2, and S_3 are the incident beam's Stokes parameters, which are related to the BCP matrix by $S_0=j_{\text{in}}^{RR}+j_{\text{in}}^{LL}$, $S_1=j_{\text{in}}^{RL}+j_{\text{in}}^{LR}$, $S_2=-i(j_{\text{in}}^{RL}-j_{\text{in}}^{LR})$, and $S_3=j_{\text{in}}^{RR}-j_{\text{in}}^{LL}$ for $\boldsymbol{\rho}_1=\boldsymbol{\rho}_2$. To retrieve the Stokes parameters, two different measurements are required. The first is obtained by orienting the polarizer at 0° and capturing all three intensity spots, I_1, I_{-1}, $I_0(\gamma=0°)$, whereas we obtain the second by orienting the polarizer at 45° and analyzing only the central spot, $I_0(\gamma=45°)$.

To test our polarimeter we obtained a DSG element by using advanced photolithographic techniques.[7] The DSG element, which was designed for CO_2 laser radiation of 10.6 μm wavelength, was fabricated upon a 500 μm thick GaAs wafer with a subwavelength period of $\Lambda=2$ μm and grating period $d=2.5$ mm. The DSG's groove orientation is actually a discrete function, $F[\theta(\xi)]$. This design procedure yields a 98.7% diffraction efficiency for the first diffracted order when 16 discrete levels are used.[6] The dimensions of the element were 25 mm × 3 mm and consisted of 10 periods of d. Figure 1(b) shows a scanning-electron-microscope image of a region upon the DSG, while Fig. 1(c) shows an image of a cross section of the subwavelength grooves.

We used the setup depicted in Fig. 1 to test our concept for polarization measurement, where the focal length of the lens was $f=1$ m and the actual aperture was limited by the DSG. First, we measured the birefringent values of the DSG to be $t_x=0.85$, $t_y=0.75$, and $\phi=101°$.[7] The measured values were close to the theoretical prediction achieved by using rigorous coupled-wave analysis calculated for the groove shape depicted in Fig. 1(c).

Next, to demonstrate the ability to measure fully polarized light, we illuminated the polarimeter with a linearly polarized CO_2 laser beam with a wavelength of 10.6 μm followed by a rotating QWP. The rotating QWP was used as a polarization-state generator. The far-field intensities were captured by a Spiricon Pyrocam III camera. In the case of fully po-

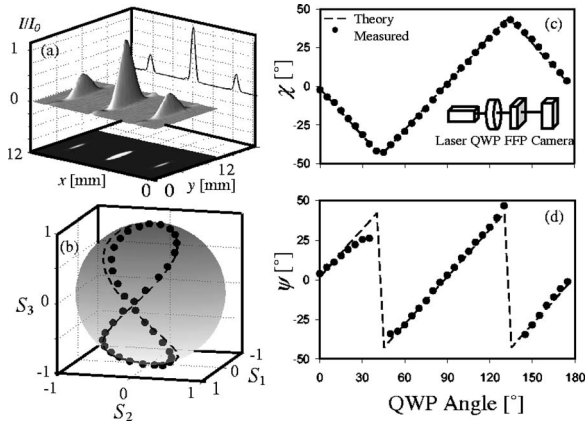

Fig. 2. (a) Measured intensity in the focal plane of a beam emerging from a DSG followed by a polarizer oriented at 0°. (b) Measured (squares) and predicted (dashed curve) polarization states of a rotating QWP depicted on a Poincaré sphere. Measured (circles) and predicted (solid curves) values for (c) ellipticity angle χ and (d) azimuthal angle ψ as functions of the orientation of the QWP. The inset in (c) shows the setup for generating fully polarized light by use of a rotating QWP. FFP, the far-field polarimeter.

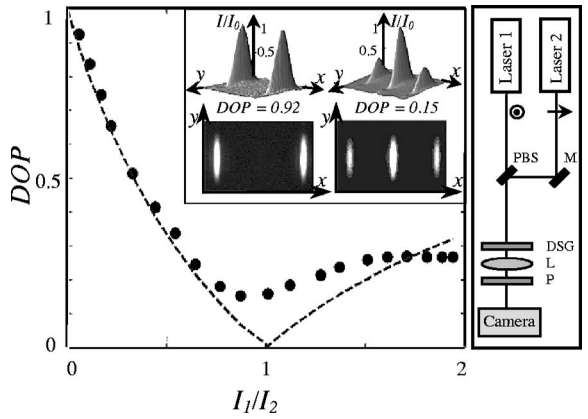

Fig. 3. Calculated (dashed curve) and measured (circles) DOPs as functions of the intensity ratio of the two independent lasers that have orthogonal linear polarization states. The inset at the right shows the setup for combining the two lasers to generate partially polarized light. PBS, polarization beam splitter; M, mirror; L, lens; P, polarizer. Also shown are the experimental intensity distributions for DOPs of 0.15 and 0.92.

larized light, measurement with a single polarizer orientation angle is sufficient, in which three Stokes parameters are retrieved and the fourth parameter is calculated by use of the relation $S_0^2=S_1^2+S_2^2+S_3^2$. Figure 2(a) shows the measured intensity distribution captured in a single camera frame when the fast axis of the QWP was set at a 0° angle and the polarizer, placed at the focal plane, was oriented at 0°. Figure 2(b) shows the measured and predicted Stokes parameters on a Poincaré sphere for the analyzed incident beam. This figure provides a graphic representation that shows all four Stokes parameters simultaneously, thereby emphasizing the good agreement between the predicted and measured values for polarized light. Moreover, Figs. 2(c) and 2(d) show the experimental and theoretical ellipticity, χ, and azimuthal angle, ψ, calculated from the data in Fig. 2(b) by use of the relations $\tan(2\psi)=S_2/S_1$ and $\sin(2\chi)=S_3/S_0$. The measurements yielded standard deviation errors with respect to the theoretical prediction of 1.73° and 0.95° for the azimuthal angle and the ellipticity, respectively. The errors in the polarization measurements result mainly from spatial inhomogeneity of the QWP retardation, which is ±2°, but also from statistical noise arising from spatial and temporal fluctuations of the light emitted from the laser and from shot noise and amplifier noise of the IR camera.

To demonstrate the use of our polarimeter for partially polarized beams, we combined two independent CO_2 lasers in orthogonal linear polarization states by use of the setup depicted in Fig. 3. The degree of polarization (DOP) is defined by $\mathrm{DOP}=(S_1^2+S_2^2+S_3^2)^{1/2}/S_0$. For two orthogonal, linearly polarized beams, the DOP is $(I_1-I_2)/(I_1+I_2)$, where I_1 and I_2 are the intensities of the horizontally and vertically polarized beams, respectively. For partially polarized beams two different measurements are required, which we can obtain by orienting the polarizer at 0° and 45°. Figure 3 shows the measured and predicted DOPs as a function of intensity ratio I_1/I_2. The inset shows the experimental intensity distributions for two extreme cases analyzed by a polarizer oriented at 0°. The first distribution is for equal intensities ($I_1=I_2$), in which the measured DOP is 0.15, indicating unpolarized light. The second is for illumination by a single laser only (i.e., $I_2=0$), in which the measured DOP is 0.92, indicating fully polarized light. This experiment shows the ability to obtain all four Stokes parameters.

E. Hasman's e-mail address is mehasman@tx.technion.ac.il.

References

1. G. P. Nordin, J. T. Meier, P. C. Deguzman, and M. W. Jones, J. Opt. Soc. Am. A **16**, 1168 (1999).
2. R. M. A. Azzam, Opt. Lett. **12**, 555 (1987).
3. A. De Martino, E. Garcia-Caurel, B. Laude, and B. Drévillon, Thin Solid Films **455-456**, 112 (2004).
4. F. Gori, Opt. Lett. **24**, 584 (1999).
5. E. Hasman, G. Biener, A. Niv, and V. Kleiner, "Space-variant polarization manipulation," in *Progress in Optics*, E. Wolf, ed. (Elsevier, 2005), Vol. 47.
6. E. Hasman, V. Kleiner, G. Biener, and A. Niv, Appl. Phys. Lett. **82**, 328 (2003).
7. G. Biener, A. Niv, V. Kleiner, and E. Hasman, J. Opt. Soc. Am. A **20**, 1940 (2003).
8. F. Gori, M. Santarsiero, R. Borghi, and G. Piquero, Opt. Lett. **25**, 1291 (2000).
9. L. Mandel and E. Wolf, *Optical Coherence and Quantum Optics* (Cambridge U. Press, 1995).